Journal of Polymer Research (2022) 29:337
https://doi.org/10.1007/s10965-022-03190-4

ORIGINAL PAPER

Fabrication of rechargeable proton battery and PEM fuel cell using biopolymer Gellan gum incorporated with NH_4HCO_2 solid electrolyte

Meera Naachiyar R[1,2] · Ragam M[1] · Selvasekarapandian S[2,3] · Aristatil G[2] · Aafrin Hazaana S[1,2] · Muniraj Vignesh N[2,4] · Vengadesh Krishna M[2,5]

Received: 23 March 2022 / Accepted: 8 July 2022

Abstract

Solid electrolyte for electrochemical device applications have been developed using a linear anionic polysaccharide, Gellan gum incorporated with Ammonium formate (NH_4HCO_2) by the solution casting technique using double distilled water as solvent. The amorphous nature and the crystallinity percentage of the polymer membranes have been calculated from X-ray Diffraction (XRD) technique and the complex formation between the polymer and salt have been studied using Fourier transform infrared (FTIR) technique. Ionic conductivity of developed membranes has been found by measuring its impedance. Polymer membrane (1 g Gellan gum: 0.9 M.wt % of NH_4HCO_2) exhibits the conductivity of $5.62 \pm 0.09 \times 10^{-3}$ S/cm. The Differential Scanning Calorimetric (DSC) thermograms have been used to study the glass transition temperature in the membranes. The predominant transportation of ions has been proved by DC Wagner's Polarization technique. The electrochemical stability for the highest ion conducting polymer membrane has been studied using Linear sweep Voltametry (LSV). Using highest conducting polymer membrane as an electrolyte, the electrochemical devices – primary battery, rechargeable battery and proton exchange membrane (PEM) fuel cell have been constructed and their performance has been analyzed. The primary battery exhibited the open circuit voltage (OCV) of 1.78 V, the rechargeable battery provided the highest potential of 2.27 V and the PEM fuel cell exhibits the OCV of 763 mV.

Keyword Gellan gum · Ammonium formate · Rechargeable proton battery · PEM fuel cell

Introduction

Electrochemical devices like laptop computers, cell phones etc. demand efficient, sustainable, harmless and eco-friendly energy storage devices. The battery is one of the efficient, commercial energy storage devices which comprises of anode, cathode and electrolyte. One of the components namely electrolyte plays a vital role in the performance of the battery. Among various electrolytes such as liquid, gel and solid electrolyte, solid polymer electrolytes are preferred due to practical advantages over liquid electrolyte.

The preference towards the solid polymer electrolyte in the electrochemical device is due to their efficient advantages like their electrochemical stability, lightweight and flexible property, their film-forming ability and no leakage property. [1–4]. Different methods such as blending of two polymers, addition of inorganic fillers or plasticizers enhance the properties of an electrolyte.

Various polymeric systems based on synthetic polymers such as PVA, PVP, PAN, PMMA, PVC etc. are used as electrolytes. Even though synthetic polymers are efficient, they are not cost-effective and eco-friendly that leads to the search of effective biopolymer. Biopolymers are abundant in nature, low cost and environmental friendly. They have been reported with very good electrical properties such as ionic conductivity [4–7]. Biopolymers such as starch, cellulose, chitosan, pectin, carrageenan, agar–agar etc. have been reported earlier for energy storage.

✉ Selvasekarapandian S
sekarapandian@rediffmail.com

1 Department of Physics, Fatima College, Madurai, Tamil Nadu, India

2 Materials Research Center, Coimbatore, Tamil Nadu, India

3 Department of Physics, Bharathiar University, Coimbatore, Tamil Nadu, India

4 Department of Physics, Mannar Thirumalai Naicker College, Madurai, Tamil Nadu, India

5 Department of Chemistry, Bharathiar University, Coimbatore, Tamil Nadu, India

Published online: 18 July 2022

Gellan gum (GG), a linear anionic heteropolysaccharide has tetra-saccharide repeating units each consisting of beta-D-glucose (Glc), beta-D-glucuronic acid (GlcA) and alpha-L-rhamnose (Rha) in the ratio 2:1:1 (Fig. 1). This GG polysaccharide is produced by the bacteria named *Sphingomonas Elodea* by fermentation process. GG can produce a low viscous solution of 0.031 Pa.s. that has high thermal stability and thermal reversibility [8–11]. It has an easy film-forming tendency and a good amount of polar groups [6]. These polar groups, along with the cation of any salt, will increase the charge carrier. Hence, the biopolymer GG is chosen as the host polymer.

Consequently, ion-conducting highly transparent and temperature stable membrane is obtained and it is helpful in the field of ophthalmology for the development of lenses and currently in the electrochemical devices too. It is used as a gelling agent and possesses no danger to humans; hence it is used in food industries as food thickeners and stabilizers [11].

GG could be the best replacer in biopolymer electrolytes in commercial electrochemical devices due to its biodegradable nature, less toxic and harmless nature. It is a hot water-soluble polymer. It dissolves in water above 70ºC [6, 8–14]. Reports on GG are very sparse. Majid et al. [8] reported the highest conductivity of 5.6×10^{-6} S/cm for low acyl Gellan gum/polyvinyl pyrrolidone with the Lithium perchlorate salt. Noor et al. [9, 10] reported that the biopolymer Gellan gum with Lithium triflate shows the highest conductivity of 5.4×10^{-4} S/cm. The biopolymer Gellan gum mixed with choline-based Ionic Liquid (IL) N, N, N-trimethyl-N-(2-hydroxyethyl) ammonium bis(trifluoromethylsulfonyl) imide ($[N_{1112(OH)}][NTf_2]$) exhibits 5.2×10^{-6} S/cm, reported by Neto et al. [11]. Naachiyar et al. [6] reported the highest conductivity 1.41×10^{-2} S/cm for Gellan gum incorporated with Ammonium thiocyanate salt.

Ammonium salt has been reported as good proton donors [6]. Hence in this present work, Ammonium formate (NH_4HCO_2) salt is used to enhance the conducting nature of the Biopolymer GG. Few reports on ammonium based salt membranes are listed below.

S. Monisha et al. reported the biopolymer cellulose acetate with ammonium nitrate [15] showing conductivity of about 1.46×10^{-3} S/cm. V. Moniha et al. reported the biopolymer iota-carrageenan with ammonium formate [16] shows the ionic conductivity of 1.11×10^{-3} S/cm respectively. S. Karthikeyan has reported the conductivity of 1.46×10^{-5} S/cm for iota-carrageenan with ammonium bromide [17]. G. Boopathi et al. have reported the conductivity of about 6.57×10^{-4} S/cm for biopolymer agar–agar with ammonium nitrate salt [18]. S. Selvalakshmi et al. have reported the conductivity for Agar–agar biopolymer with ammonium iodide salt as 1.20×10^{-4} S/cm [19] and Agar–agar biopolymer with ammonium bromide as 1.33×10^{-4} S/cm [20]. Premalatha et al. have reported highest conductivity of 1.58×10^{-3} S/cm and 1.23×10^{-3} S/cm observed for tamarind seed polysaccharide with ammonium bromide [21] and tamarind seed polysaccharide with ammonium formate [22] respectively. Mohamed et al. have reported the conductivity of 1.30×10^{-4} for the starch-chitosan blend with Ammonium thiocyanate [23].

This present work aims to enhance the conductivity of the biopolymer GG membrane with NH_4HCO_2 salt and use it as an electrolyte for various electrochemical devices. In the present work, the prepared membranes have been characterized by.

- Powder XRD to study the crystalline/amorphous nature of the membranes.
- FTIR technique to confirm the complex ion formation between the polymer and salt matrix.
- Ac Impedance technique to measure the ionic conductivity of the biopolymer membranes.
- DSC analysis to study the variation in glass transition temperature for variation in ionic salt concentration.
- TGA to study the thermal stability of the highest proton conducting membrane.

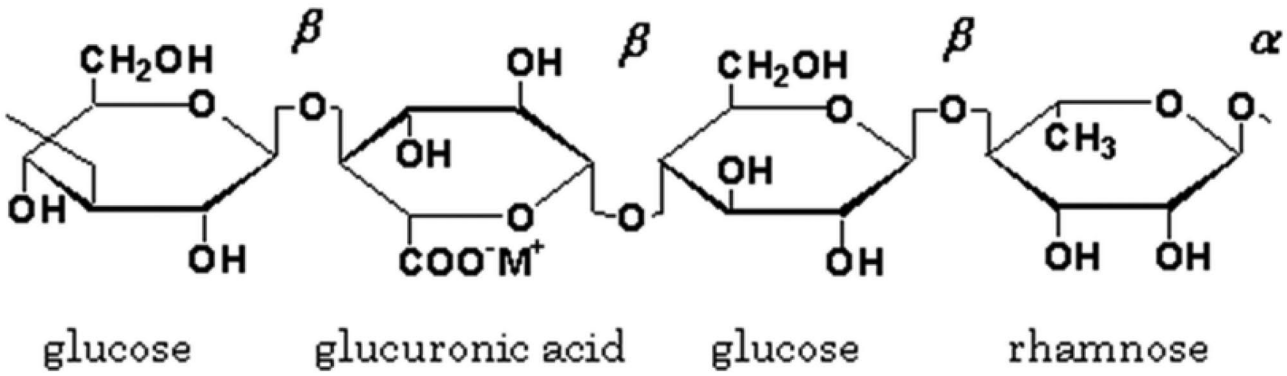

Fig. 1 Chemical structure of the biopolymer Gellan gum (GG)

- LSV to study the electrochemical stability the highest proton conducting membrane.
- Transference number measurement to study the nature of ion involved.
- Oxidative test to analyze the chemical stability of the highest proton conducting membrane.
- Mechanical test to study the mechanical strength of the highest proton conducting membrane.
- Ion exchange test to measure the ion exchange capacity value of the highest proton conducting membrane.

Primary proton battery, rechargeable proton battery and PEM fuel cell have been fabricated and their performances are studied.

Experimental technique

Materials used

- Biopolymer Gellan gum (Sisco Research Laboratories Pvt. Ltd.) – host polymer
- Ammonium formate (NH_4HCO_2) extra pure (Sisco Research Laboratories Pvt. Ltd.) – salt
- Double distilled hot water – solvent
- Ferrous sulphate ($FeSO_4$) (Sigma Aldrich Pvt. Ltd.)
- Hydrogen peroxide (H_2O_2) 30% (Merck Life Science Pvt. Ltd.)
- Sodium chloride (NaCl) (Sigma Aldrich Pvt. Ltd.)
- Sodium hydroxide (NaOH) (Sigma Aldrich Pvt. Ltd.)

Method of preparation

The membranes are prepared using the solution casting technique. The biopolymer GG is dissolved in the hot double distilled water. The gelling temperature of the GG is 30–40 ºC. So to maintain the aqueous form and avoid gel formation, the double distilled water is heated to 90 ºC and the Gellan gum is dissolved thoroughly in it. The NH_4HCO_2 salt is added to 1 g biopolymer GG in various concentrations (0.6, 0.7, 0.8, 0.9, 1.0 M.wt %). The solutions with various compositions are poured into the polypropylene petri dishes, kept in the hot air oven and dried at 70 ℃ for 12 h. Free-standing transparent membranes of thickness 0.2 mm have been obtained.

Characterization techniques

XRD

The amorphous/crystalline nature of the membrane has been studied using the X'Pert PRO diffractometer at the angle $2\theta = 5\text{-}80^{\circ}$ at the rate of 2º/min using Cu-Kα radiation operated at 40 kV/30 mA.

FTIR

SHIMADZU-IR Affinity-1 Spectrometer is used to recorded FTIR spectra in the range 500–4000 cm^{-1} with the resolution of 1 cm^{-1} at ambient temperature.

Impedance study

Using HIOKI-3532 LCR HiTester instrument with stainless steel sample holder, Ac impedance study is carried out for the prepared polymer membranes in the frequency range 42 Hz to 5 MHz.

DSC

The glass transition temperature of the polymer membrane is found using DSC Q20 V24.11 Build 124 instrument under Nitrogen atmosphere, in the temperature range from 20 ºC to 200 ºC with the heating rate of 10 ºC/min.

TGA

Thermal stability of the biopolymer membranes have been studied using the NETZSCH STA 449F3 STA449F3A-1100-M under nitrogen atmosphere. The samples were heated from the range 30 ℃ to 550 ℃ with 10 K/min.

LSV

Using the Biological Science Instrument VSP 300, France, the LSV measurement of polymer membranes is done by placing the membrane between two stainless steel electrodes, with the scan rate of 1 mV/s in the range of 0–5 V.

Transference number measurement

The ion contribution to the total electric current is identified using the transference number. The very simplest technique used to calculate the ionic transference number is Wagner's Polarization method with stainless steel electrodes.

Chemical stability test

The highest proton conducting biopolymer membrane has been treated for oxidative test by immersing the membrane in Fenton's reagent (2 ppm $FeSO_4$ in 3% H_2O_2 solution) at 80 ℃. The stability of the membrane has been evaluated based on the weight of the membrane before immersion

and residual weight after immersion in the Fenton's reagent for 1 h and the time taken for the membrane to dissolve completely.

Mechanical test

Tensile strength of the highest proton conducting membrane has been measured using Zwick-Roell Z010 Universal Testing Machine with 10 kN to find the mechanical property of the membrane. The membrane of dimension of 10 × 2 cm has been taken and the testing elongation rate was 2 mm/min.

Ion exchange capacity

Ion Exchange Capacity (IEC) of the prepared highest proton conducting biopolymer membrane has been measured using the acid–base titration method. The weight of the dry membrane has been measured and soaked in 20 ml of 1 M NaCl solution for 24 h for the exchange of H^+ ions with Na^+ ions. The obtained solution was titrated using the 0.1 M NaOH solution with phenolphthalein as an indicator and the IEC value has been obtained.

Device fabrication

Primary battery construction

Using the configuration, $Zn + ZnSO_4.7H_2O + C$ || highest conducting polymer membrane (as electrolyte) || $PbO_2 + V_2O_5 + C$, primary solid-state proton-conducting battery has been fabricated. And their performance has been studied with the load of 100 kΩ.

Rechargeable proton battery construction

The rechargeable proton battery has been constructed using the configuration, $Zn + ZnSO_4.7H_2O + C$ || highest conducting polymer membrane (as electrolyte) || $MnO_2 + C$. The cell has been charged for 2 h with DC voltage of 3 V and allowed to discharge for 2 h. The performance of the battery is studied by the charging and discharging the cell with various loads connected across them to study their voltage discharge characteristics and their corresponding current variation.

PEM fuel cell construction

Normally the membrane electrode assembly (MEA) for proton exchange membrane (PEM) fuel cell is prepared with high temperature and pressure. Since we do not have the facility to prepare MEA, a single stack PEM fuel cell has been constructed with the hand tightened method using the highest conducting biopolymer membrane as electrolyte and Platinum (Pt) coated carbon cloth as electrodes. The performance with various loads has been investigated. The results of Nafion™ 212 membrane has been compared at the same condition.

Results and discussion

XRD

The crystalline/amorphous nature of the biopolymer membrane is studied by X-ray diffraction analysis. Figure 2 represents the XRD pattern of Pure GG and 1 g GG with various M.wt % (0.6, 0.7, 0.8, 0.9 and 1.0) of NH_4HCO_2.

The intense peaks at angle 2θ = 6°, 10°, 19° and 22° are observed for the pure GG membrane. These peak values are in agreement with earlier report [2, 5, 6]. The XRD pattern of 1 g GG with different concentrations (0.6, 0.7, 0.8, 0.9, 1.0 M.wt %) of NH_4HCO_2 salt exhibits peaks at angle 2θ = 6°, 11°, 18°,

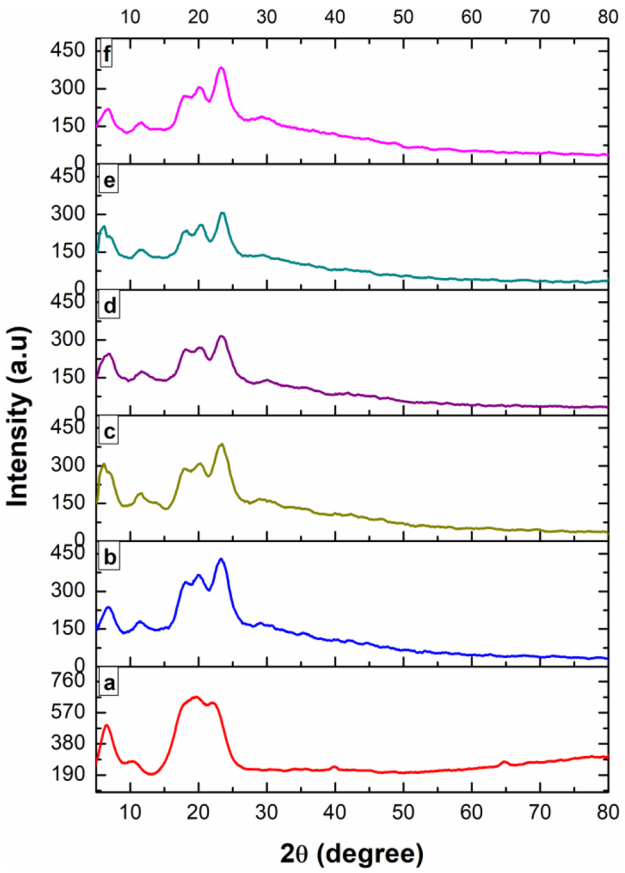

Fig. 2 XRD pattern of **a** Pure GG **b** 1 g GG: 0.6 M.wt % of NH_4HCO_2 **c** 1 g GG: 0.7 M.wt % of NH_4HCO_2 **d** 1 g GG: 0.8 M.wt % of NH_4HCO_2 **e** 1 g GG: 0.9 M.wt % of NH_4HCO_2 **f** 1 g GG: 1.0 M.wt % of NH_4HCO_2

20º and 22º. The peaks 6º, 11º, 18º, 20º and 22º exhibit decrease in intensity and increase in broadness for the increase in salt concentrations (i.e.) for 1 g GG: 0.6 M.wt % of NH_4HCO_2, 1 g GG: 0.7 M.wt % of NH_4HCO_2, 1 g GG: 0.8 M.wt % of NH_4HCO_2 and 1 g GG: 0.9 M.wt % of NH_4HCO_2 respectively. This indicates the increase in the amorphous nature of the biopolymer membrane on the addition of salt. On the addition of salt to the polymer, the systematic arrangement in the polymer matrix is disturbed and hence the increase in amorphous nature of the membranes [5].

For the composition 1 g GG: 1.0 M.wt % of NH_4HCO_2, the peaks 6º, 11º, 18º, 20º and 22º exhibit a slight increase in intensity and decrease in broadness. This result conveys the inability of the polymer matrix to hold more salt [5]. This shows a decrease in the amorphous nature of the biopolymer membrane due to the aggregate formation of the ions. Among all the biopolymer membranes, 1 g GG: 0.9 M.wt % of NH_4HCO_2 composition shows high amorphous nature.

The results of intensity and broadness of the biopolymer electrolyte membranes are in accordance with the Hodge et al. criteria [24]. No peaks of NH_4HCO_2 salt are found in the salt-added polymer matrix. This indicates the complete dissociation of NH_4HCO_2 salt.

Crystallinity percentage calculation

Figure S1 shows the deconvoluted XRD pattern of Pure GG and 1 g GG with various M.wt % (0.6, 0.7, 0.8, 0.9 and 1.0) of NH_4HCO_2. Table S1 shows the Crystallinity percentage of the Pure GG and 1 g GG with various M.wt % (0.6, 0.7, 0.8, 0.9 and 1.0) of NH_4HCO_2.

$$Percentage\ of\ Crystallinity(\%C) = \frac{Area\ under\ crystalline\ region}{Total\ area\ of\ the\ peak} \times 100\%$$

Using the above equation, the percentage of crystallinity has been calculated from the deconvoluted graph.

From the Table S1, it is observed that the crystallinity percentage of the Pure GG is 33.76%. On addition of 0.6, 0.7, 0.8 and 0.9 M.wt % of NH_4HCO_2 with 1 g GG, the crystallinity percentage decrease to 27.06%, 16.19%, 10.25% and 7.12% respectively. The amorphous nature of the GG biopolymer membrane increases as the salt concentration increases. While adding 1.0 M.wt % of NH_4HCO_2 with 1 g GG, the percentage of crystallinity increases to 11.26%. Biopolymer membrane, 1 g GG: 0.9 M.wt % of NH_4HCO_2 shows high amorphous nature.

FTIR

Figure S2 shows the FTIR spectra of Pure GG and 1 g GG with various M.wt % (0.6, 0.7, 0.8, 0.9 and 1.0) of NH_4HCO_2.

The IR peak at 1038 cm^{-1} for pure GG membrane is due to C-O stretching vibration [6, 10, 13], and this peak is found to be shifted to 1033 cm^{-1}, 1032 cm^{-1}, 1031 cm^{-1}, 1030 cm^{-1} and 1029 cm^{-1} for 0.6, 0.7, 0.8, 0.9 and 1.0 M.wt % of NH_4HCO_2 with 1 g GG membranes respectively.

The peak at 1420 cm^{-1} for pure GG is due to C–C stretching vibration [9, 12]. On addition of 0.6, 0.7, 0.8, 0.9 and 1.0 M.wt % of NH_4HCO_2 to 1 g GG, the peak at 1420 cm^{-1} gets shifted to 1424 cm^{-1}, 1425 cm^{-1}, 1427 cm^{-1}, 1434 cm^{-1} and 1442 cm^{-1} respectively.

The peaks 1575 cm^{-1}, 1574 cm^{-1}, 1573 cm^{-1}, 1571 cm^{-1} and 1571 cm^{-1} are observed for 0.6, 0.7, 0.8, 0.9 and 1.0 M.wt % of NH_4HCO_2 with 1 g GG membranes respectively. Literature reports [6, 25] that NH_3^+ vibration has a peak at 1575 cm^{-1}. This peak is not observed in pure GG. This confirms the complex formation between the polymer and salt matrix.

The peak located at 1636 cm^{-1} for pure GG is due to C = O stretching vibration, corresponds to glycosidic bond [6, 9, 14]. This peak has been submerged along with the peak of 1575 cm^{-1}. This also confirms the complex formation between the polymer and salt matrix.

The broad O–H stretching vibration peak is observed for pure GG at 3270 cm^{-1} [16] and it gets shifted to 3212 cm^{-1}, 3210 cm^{-1}, 3209 cm^{-1}, 3201 cm^{-1} and 3205 cm^{-1} for salt added (0.6, 0.7, 0.8, 0.9 and 1.0 M.wt % of NH_4HCO_2 with 1 g GG) GG membranes respectively.

The assignments of peaks are tabulated in Table S2. The change in peak intensity, frequency shift and appearance of the new peak depicts the complex formation between the biopolymer GG and the salt NH_4HCO_2.

The force constant, k, can be determined by the Hooke's formula,

$$\overline{\nu} = \frac{1}{2\pi c}\sqrt{\frac{k}{\mu}}\mathrm{N/cm}$$

where, $\mu = \frac{m_1 \times m_2}{m_1 + m_2}$ is the reduced mass. The force constant has been calculated for O–H stretching and C-O stretching and tabulated in Table S3. The force constant values have been changed for the NH_4HCO_2 added GG membranes. This indicates the interaction of salt with the polymer matrix resulting in bond length variation. As the salt concentration increases, the force constant decreases hence the bond length increases with decrease in frequency. The possible interaction of NH_4HCO_2 with the GG is shown in Fig. S3.

DSC

Figure 3 depicts the DSC thermograms of the Pure GG and 1 g GG with various M.wt % (0.6, 0.7, 0.8, 0.9 and 1.0) of NH_4HCO_2 salt. The glass transition temperature (T_g) of the biopolymer membrane is calculated using the DSC analysis.

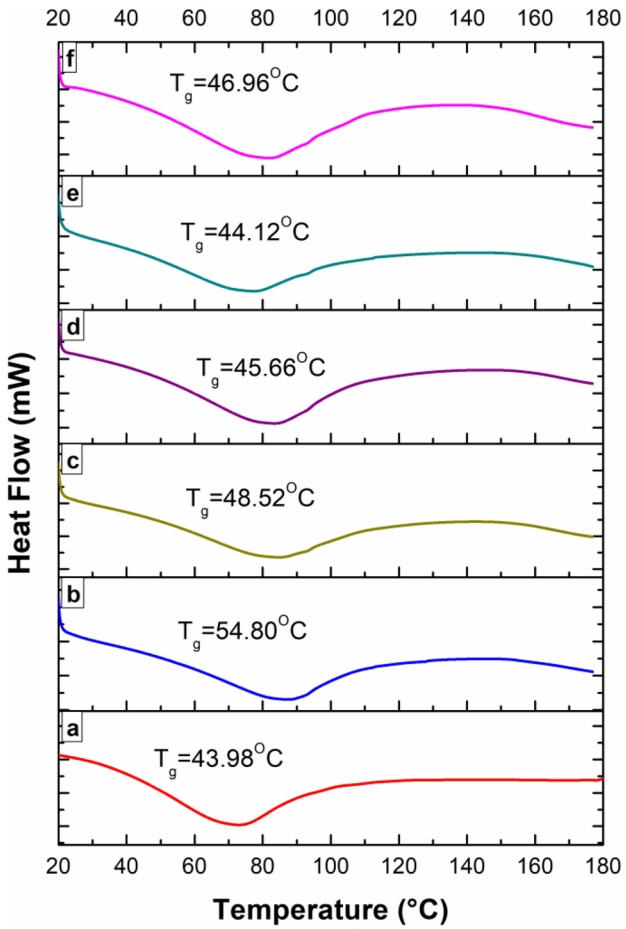

Fig. 3 DSC thermograms of **a** Pure GG **b**1 g GG: 0.6 M.wt % of NH_4HCO_2 **c**1 g GG: 0.7 M.wt % of NH_4HCO_2 **d**1 g GG: 0.8 M.wt % of NH_4HCO_2 **e**1 g GG: 0.9 M.wt % of NH_4HCO_2 **f**1 g GG: 1.0 M.wt % of NH_4HCO_2

The Pure GG shows the T_g value of 43.98 ºC. Addition of 0.6 M.wt % of NH_4HCO_2 salt with 1 g GG, the T_g value increase to 54.80 ºC. This increase in T_g value is due to the strong transient cross-linkage between the oxygen atom and H^+ ion [26]. This leads to the increase in stiffness of the polymer chain. Further, on the addition of 0.7 M.wt % of NH_4HCO_2, 0.8 M.wt % of NH_4HCO_2 and 0.9 M.wt % of NH_4HCO_2 salt with 1 g GG, the T_g value decrease to 48.52 ºC, 45.66 ºC and 42.12 ºC respectively. This indicates the weak transient cross-linkage between the oxygen and H^+ ion which leads to the softening of the polymer chain [26]. Further on the addition of 1.0 M.wt % of NH_4HCO_2 salt with 1 g GG, the T_g value again increased to 46.96 ºC. The composition 0.9 M.wt % of NH_4HCO_2 salt with 1 g GG membrane shows the T_g value 42.12 ºC. This value is less than the Pure GG sample. Low T_g value makes the membrane more flexible. Due to the agglomeration of more salt in the polymer chain matrix for the membrane of composition, 1.0 M.wt % of NH_4HCO_2 salt with 1 g GG gets stiffened which leads to increase of T_g value. The T_g values of the Pure GG and 1 g GG with various M.wt % (0.6, 0.7, 0.8, 0.9 and 1.0) of NH_4HCO_2 salt are tabulated in Table 1.

Ac impedance spectroscopy study

Nyquist-plot

Figure 4i, ii show the Nyquist plot of the pure GG and 1 g GG with various M.wt % (0.6, 0.7, 0.8, 0.9 and 1.0) of NH_4HCO_2 at room temperature

Usually, the Nyquist plot, also called the cole–cole plot, shows a depressed semicircle followed by an inclined line for the graph plot between the real (Z') and the imaginary part (Z") of the impedance. The depressed semicircle that appears at the high-frequency region is due to parallel combination of bulk resistance and bulk capacitance and the inclined line that appears at the low-frequency region is because of electrode–electrolyte interface. Due to the addition of salt, the semicircle vanishes (Fig. 4ii) in the cole–cole plot.

The equivalent circuits are shown in Figs. 4i, ii. The bulk resistance (R_b) of the polymer membranes is calculated using the Boukamp EQ software [27]. The Ionic conductivity of polymer membranes at room temperature are calculated using the formula,

$$\sigma = \frac{l}{AR_b} \mathrm{S/cm}$$

where l is the thickness, A is the area and R_b is the bulk resistance of the biopolymer membrane.

As seen from the Table 2, it is noted that, conductivity values increases, as the salt concentration increases. The conductivity is maximum for biopolymer 1 g GG with 0.9 M.wt % of NH_4HCO_2. This membrane is more amorphous (as confirmed from XRD) and it has low T_g value (from DSC). Low T_g leads to flexibility of the membrane and hence the conductivity has been increased.

Also it is observed that, the R_b values decrease with increase in salt concentration. The R_b value for 0.6, 0.7, 0.8 and 0.9 M.wt % of NH_4HCO_2 with 1 g GG are 1646 Ω, 6.242 Ω, 1.879 Ω, 1.470 Ω, 1.157 Ω and 1.275 Ω respectively. The impedance of the constant phase element (CPE) is given by the equation,

$$Z_{CPE} = \frac{1}{Q_0 j\omega^n}$$

where Q_0 and n are frequency-independent factors. The CPE value for 0.6, 0.7, 0.8 and 0.9 M.wt % of NH_4HCO_2 with 1 g GG are 30, 141, 121, 120, 79 and 339 respectively. If n = 1, it is pure capacitor and n = 0, it is pure resistor. In this research

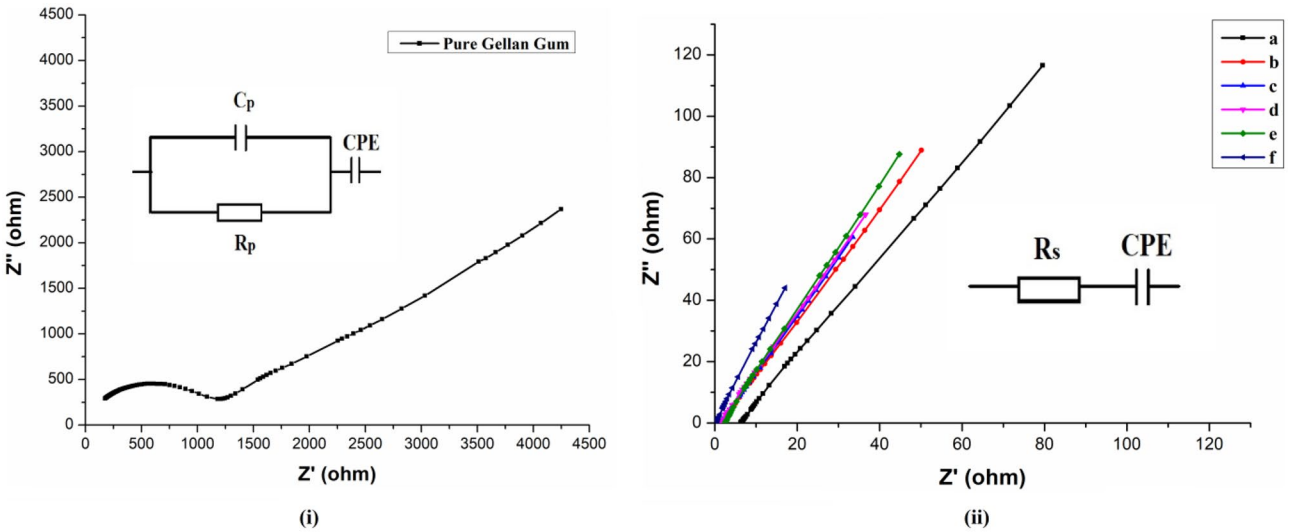

Fig. 4 Nyquist plot for **i** pure GG and **ii** 1 g GG with various compositions of NH_4HCO_2 **a**1 g GG: 0.6 M.wt % of NH_4HCO_2 **b**1 g GG: 0.7 M.wt % of NH_4HCO_2 **c**1 g GG: 0.8 M.wt % of NH_4HCO_2 **d**1 g GG: 0.9 M.wt % of NH_4HCO_2 **e**1 g GG: 1.0 M.wt % of NH_4HCO_2

work n varies from 0 to 1. The n value for 0.6, 0.7, 0.8 and 0.9 M.wt % of NH_4HCO_2 with 1 g GG are 0.499, 0.661, 0.716, 0.721, 0.783 and 0.515 respectively.

For 1.0 M.wt % of NH_4HCO_2 with 1 g GG, the conductivity decreases to $2.34 \pm 0.12 \times 10^{-3}$ S/cm. The EIS measurement has been carried out at the room temperature. V. Moniha et al. reported that the conducting biopolymer iota-carrageenan with ammonium nitrate [15] and iota-carrageenan with ammonium formate [16] reported conductivity of 1.46×10^{-3} S/cm and 1.11×10^{-3} S/cm respectively. Premalatha et al. have reported highest conductivity of 1.58×10^{-3} S/cm and 1.23×10^{-3} S/cm observed for tamarind seed polysaccharide with ammonium bromide [21] and tamarind seed polysaccharide with ammonium formate [22] respectively.

Conductance spectra

Figure S4 shows the graphical plot between frequency and logarithmic conductivity for Pure GG and 1 g GG with various M.wt % (0.6, 0.7, 0.8, 0.9 and 1.0) of NH_4HCO_2 at the room temperature. Fig. S4 shows the presence of low-frequency dispersive region and mid-frequency plateau region. This gives the dc conductivity (σ_{dc}) value by extrapolating the plateau region to the log σ axis. The value obtained from the Nyquist is well in accordance with the conductance spectra for the pure GG and 1 g GG with various M.wt % (0.6, 0.7, 0.8, 0.9 and 1.0) of NH_4HCO_2.

Generally, the conductance spectra possess three regions: (a) low-frequency dispersion region – performed at blocking electrode due to the space charge polarization, (b) frequency-independent region – dc conductivity of the polymer complex is studied and (c) dispersive high-frequency region – shows the increase in conductivity. In this work, low frequency and frequency independent regions are only observed.

Table 1 DSC thermograms of 1 g GG with various M.wt % of NH_4HCO_2 salt

COMPOSITION	T_g(℃)
Pure Gellan gum	43.98
1 g Gellan gum: 0.6 M.wt % of NH_4HCO_2	54.80
1 g Gellan gum: 0.7 M.wt % of NH_4HCO_2	48.52
1 g Gellan gum: 0.8 M.wt % of NH_4HCO_2	45.66
1 g Gellan gum: 0.9 M.wt % of NH_4HCO_2	44.12
1 g Gellan gum: 1.0 M.wt % of NH_4HCO_2	46.96

TGA

Figure S5 shows the thermo gravimetric analysis of the pure GG, the highest proton conducting membrane (1 g GG: 0.9 M.wt % of NH_4HCO_2) and Nafion™ 212 membranes.

Initial weight loss of pure GG, highest proton conducting membrane (1 g GG: 0.9 M.wt % of NH_4HCO_2) and Nafion™ 212 membrane are 12.34%, 27.03% and 4.42% respectively in the temperature range 50 ℃ to 200 ℃ (for pure GG), 30 ℃ to 110 ℃ (for the highest proton conducting membrane (1 g GG: 0.9 M.wt % of NH_4HCO_2)) and 30 ℃ to 285 ℃ (for Nafion™ 212 membrane) respectively. This initial weight loss is due to the evaporation of moisture in all the membranes. The moisture content in the highest proton conducting membrane (1 g GG: 0.9 M.wt % of NH_4HCO_2)

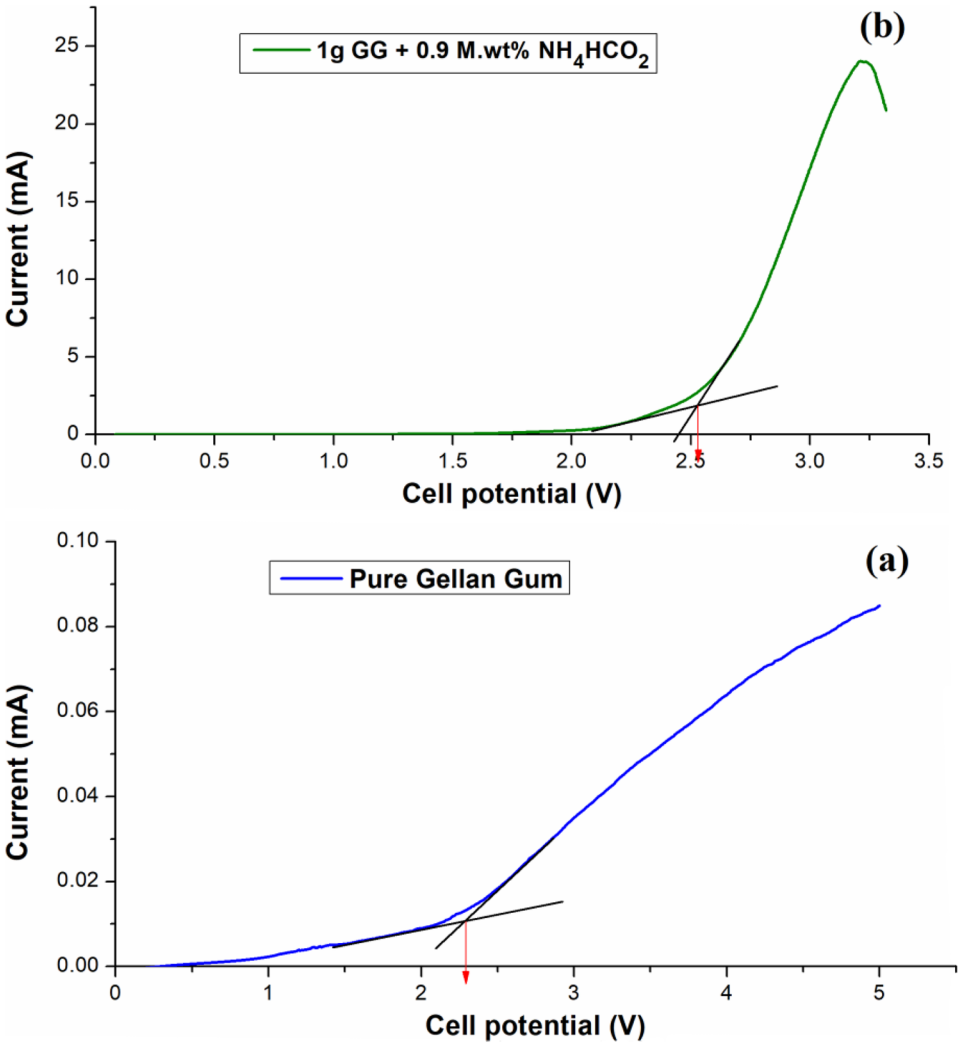

Fig. 5 **a** LSV of Pure GG and **b** 1 g GG: 0.9 M.wt % of NH_4HCO_2 (highest conducting electrolyte)

is comparatively higher than the pure GG membrane. This is due to the hydrophilic property of salt [9, 13].

The first step of degradation starts for pure GG from 200 ℃ to 260 ℃ with the weight loss of 40.23% followed by the second step of degradation from 260 ℃ to 470 ℃ resulting in 16.48% weight loss. This is due to the polysaccharide backbone degradation in the GG polymer [9, 13]. Similarly for the highest proton conducting membrane (1 g GG: 0.9 M. wt % of NH_4HCO_2), the first step of degradation starts from 110 ℃ to 244 ℃ with the weight loss of 32.32% followed by the second step of degradation from 244 ℃ to 280 ℃ resulting in 15.08% weight loss. This is due to the degradation of polymer-salt matrix. During the degradation process the polymer membrane suffers endothermic reaction of oxidation and hydrolysis subsequently the exothermic reaction of polysaccharide pyrolysis [9, 28]. The remaining residue of 19.95% for pure GG and 7.61% for highest proton conducting membrane (1 g GG: 0.9 M.wt % of NH_4HCO_2) have been obtained.

The Nafion™ 212 membrane experiences the first step of degradation from 285 ℃ to 386 ℃ with 15.26% weight loss. This is due to the degradation of sulfonic groups (that is,

Table 2 EIS parameters of biopolymer membranes

COMPOSITION	R_b (Ω)	CPE (μF)	n (no unit)	σ (S/cm)
Pure Gellan gum	1646	30	0.499	$4.22 \pm 0.14 \times 10^{-6}$
1 g Gellan gum: 0.6 M.wt % of NH_4HCO_2	6.242	141	0.661	$7.05 \pm 0.11 \times 10^{-4}$
1 g Gellan gum: 0.7 M.wt % of NH_4HCO_2	1.879	121	0.716	$3.22 \pm 0.06 \times 10^{-3}$
1 g Gellan gum: 0.8 M.wt % of NH_4HCO_2	1.470	120	0.721	$4.23 \pm 0.03 \times 10^{-3}$
1 g Gellan gum: 0.9 M.wt % of NH_4HCO_2	1.157	79	0.783	$5.62 \pm 0.09 \times 10^{-3}$
1 g Gellan gum: 1.0 M.wt % of NH_4HCO_2	1.275	339	0.515	$2.34 \pm 0.12 \times 10^{-3}$

side chains –OCF_2CF_2–SO_3H) present in the Nafion™ 212 membrane [29]. The second step of degradation from 386 ℃ to 510 ℃ resulting in the weight loss of 78.45% is due to the degradation of polymer backbone (that is main chains CF_2–CF_2) in the Nafion™ 212 membrane. The remaining residual weight results in 1.79%.

Linear sweep voltammetry

Electrochemical stability of highest conducting biopolymer electrolyte (1 g GG: 0.9 M.wt % of NH_4HCO_2) is studied using Linear Sweep Voltammetry (LSV). The electrolyte sample is placed in between two stainless steel blocking electrodes. Linear sweep voltammogram of pure Gellan Gum and the highest conducting biopolymer electrolyte sample, 1 g GG: 0.9 M.wt % of NH_4HCO_2 is shown in the Fig. 5a, b.

From the graph (Fig. 5a), it is observed that, the pure GG electrolyte is stable upto 2.28 V and decomposes further. Similarly, the composition, 1 g GG: 0.9 M.wt % of NH_4HCO_2 (Fig. 5b) shows its stability upto 2.53 V. It can be defined as, when the pure GG is incorporated with ionic salts, it offers a very good electrochemical stability. Hence, this highest conducting solid polymer biopolymer electrolyte can be a promising substitute for the practical application in electrochemical devices. Muthukrishnan et al. [30] has been reported the electrochemical window for the compositions 50 M.wt % of Pectin: 50 M.wt % of NH_4HCO_2 and 50 M.wt % of Pectin: 50 M.wt % of NH_4HCO_2: 0.4% M.wt % of EC are 1.97 V and 2.35 V.

Transference number measurement

The nature of the charge carrier in the total electric current is determined by the transference number. This transference number is measured using the simple technique known as Wagner's Polarization technique.

Here, the highest conducting biopolymer membrane (1 g GG: 0.9 M.wt % of NH_4HCO_2) is kept in between two stainless steel blocking electrodes. Later a DC voltage of 1.5 V is applied across the electrodes. As soon as the DC voltage is applied, the migration of ions results in the initial current and rapidly the current falls with time. The current value is monitored with time and their graph is drawn between current and time and it is shown in Fig. S6. The initial and final current values are noted. The transference number of ion (t_i) and electron (t_e) can be calculated from the equations below.

$$t_i = \frac{I_i - I_f}{I_i}$$

$$t_e = \frac{I_f}{I_i}$$

where t_i and t_e are the transference number of ions and electrons; I_i and I_f are the initial and final current. Using the above equations, we could infer that, $t_i = 0.95$ and $t_e = 0.05$. This shows that the conductivity is due to ions.

Chemical stability test

The oxidative stability or the chemical stability of the proton exchange membranes (PEM) are mainly studied based on their degradation nature. The degradation of the polymer membrane is mainly due to the attack of free radicals HO• and HO_2• radicals form the cathode side while performing the fuel cell operation [31, 32]. The oxidative stability of the pre-weighed highest proton conducting biopolymer membrane (1 g GG: 0.9 M.wt % of NH_4HCO_2) has been evaluated, here the membrane of dimension 2 × 2 cm has been treated with 20 ml Fenton's reagent (2 ppm $FeSO_4$ in 3% H_2O_2 solution) for 1 h at 80 ℃. The residual weight of the treated membrane after 1 h is weighed and noted and again soaked in the reagent. After 1 h, the weight loss in the membrane has been observed indicating the dissolving behavior of the membrane. The membrane began to dissolve after 1 h and completely dissolved in another 30 min.

Mechanical test

Figure S7 shows the tensile strength vs strain plot for the highest proton conducting membrane (1 g GG: 0.9 M.wt % of NH_4HCO_2). The highest proton conducting membrane (1 g Gellan Gum: 0.9 M.wt % of NH_4HCO_2) of dimension 10 × 2 cm and thickness 0.024 cm has been taken and subjected for mechanical stability test. This membrane has a good mechanical stability with a tensile strength of 20.37 ± 5 MPa and strain of 26.67 ± 7%. Pasquini et al. [33] have been reported tensile strength of 21 ± 6 MPa and strain of 245 ± 105% for Nafion™ 212 membrane.

Ion exchange capacity

Ion Exchange Capacity (IEC) of a biopolymer membrane indicates the availability of ion exchanging groups, mainly the protons which determines the ionic conductivity of membrane, by acid–base titration method [32, 34]. The highest proton conducting membrane (1 g GG: 0.9 M.wt % of NH_4HCO_2) of dimension 2 × 2 cm and weight of 0.198 g has been immersed in the 20 ml of 1 M NaCl solution for 24 h. During this 24 h, the membrane completely releases the H^+ ions and replaces them with Na^+ ions. After 24 h, the obtained solution has been titrated using 0.1 M NaOH solution with phenolphthalein as an indicator. The IEC value of highest proton conducting biopolymer membrane (1 g GG: 0.9 M.wt % of NH_4HCO_2) is measured to be 0.353 mmol/g using equation,

$$IEC\ (mmol/g) = \frac{C_{NaOH} \times V_{NaOH}}{W_{dry}}$$

where, C_{NaOH} (mol/l) is the concentration of the NaOH solution used in the titration, V_{NaOH} (ml) is the volume of the NaOH solution used while titrating against the unknown solution and W_{dry} (g) is the weight of the dry membrane before treating in NaCl solution.

Fabrication of electrochemical devices

Proton battery

A primary proton-conducting battery is fabricated using the highest conducting biopolymer membrane as the electrolyte and suitable electrodes (anode and cathode). The well grinded mixture of Zinc metal powder (Zn), Zinc Sulphate ($ZnSO_4.7H_2O$) and Graphite powder in a 3:1:1 ratio was used as the anodic material. Similarly, Lead dioxide (PbO_2), Vanadium pentoxide (V_2O_5) and Graphite powder in ratio 4:1:0.5 are grinded well and used as the cathodic material [35]. Pellets are formed from anode and cathode mixture using a pellatizer.

In between the anode and cathode pellets, the highest conducting biopolymer membrane (1 g GG: 0.9 M.wt % of NH_4HCO_2) is placed. The structure of the battery is,

$$Zn + ZnSO_4.7H_2O + C$$
$$||1g\ Gellan\ Gum + 0.9M.wt\ \%\ of\ NH_4HCO_2||PbO_2 + V_2O_5 + C$$

The anode and cathode reactions are given below.

The anode reaction is,

$$n\ Zn + ZnSO_4.7H_2O \leftrightarrow Zn_{(n+1)}SO_4.(7-2n)H_2O.2n(OH) + 2nH^+ + 2ne^-$$

The cathode reaction is,

$$PbO_2 + 4H^+ + 2e^- \leftrightarrow Pb^{2+} + 2H_2O$$

$$V_2O_5 + 6H^+ + 2e^- \leftrightarrow 2VO^{2+} + 3H_2O$$

The fabricated primary battery shows the OCV of 1.8 V (Fig. 6). When a load resistance of 100 kΩ is connected to the battery, the voltage drops to 1.78 V from 1.8 V and 17 µA current is drawn. While discharging, the voltage drop gradually and became steady at 0.93 V and observe for 60 h. The cell parameters are listed in table S4.

There are few reports on primary Proton battery. Moniha et al. have reported on iota-carrageenan with NH_4HCO_2 showing OCV of 1.56 V [16]. Maheshwari et al. have reported OCV of 1.75 V for Dextran-PVA with NH_4SCN [36]. The OCV 1.61 V and 1.78 V have been reported by Hemalatha et al. for PVA-Proline with NH_4SCN [37] and PVA-Proline with NH_4Cl [38]. Selvalakshmi et al. have reported on Agar with NH_4I showing OCV of 1.73 V [20].

Rechargeable proton battery

The rechargeable proton battery has been constructed using the electrodes, anode and cathode, coated on the current collectors copper and aluminum foil sheets and the highest conducting polymer electrolyte (1 g GG: 0.9 M.wt % of NH_4HCO_2).

The anode has been prepared using the Zinc metal powder (Zn), Zinc Sulphate ($ZnSO_4.7H_2O$) and Graphite powder in the ratio 3:1:1 and mixed in the n-methyl 2-pyrollidone (NMP) solution to form slurry. The slurry has been uniformly coated using the doctor blade over the copper foil sheet and dried in hot air oven for 30 min at 40 ℃.

Similarly, the cathode has been prepared using the Manganese Oxide (MnO_2) and Graphite powder in the ratio 3:1 and mixed in the NMP solution to form slurry and this slurry has been coated over the aluminum foil sheet uniformly using the doctor blade and allowed to dry in the hot air oven for 30 min at 40 ℃.

The dried anode and cathode were cut into required shapes and their thickness and weight has been measured. The anode, highest conducting polymer electrolyte and cathode were assembled in the battery holder as structured below.

$$Zn + ZnSO_4.7H_2O + C$$
$$||1g\ Gellan\ Gum + 0.9M.wt\ \%\ of\ NH_4HCO_2||MnO_2 + C$$

After the construction of the cell, the initial voltage has been measured at room temperature. The Impedance measurement has been taken and the cell was allowed to charge for 2 h with the DC voltage of 3 V and after that the cell was allowed to discharge for another 2 h. The output voltage has been measured. After repeating the charge and discharge cycle at room temperature for further 6 cycles (7^{th} cycle), the cell has been subjected for Impedance measurement. After continuous charge and discharge cycle, various loads such as 100 Ω, 1 kΩ, 47 kΩ and 100 kΩ have been connected respectively. Allowing the cell for charge and discharge after connecting each load, their variation in output voltage and their corresponding variation in current have been recorded. After that the Impedance measurement has been carried out. From the impedance analysis, the resistance at every interval of cycle has been studied.

The Fig. 7a represents the charge and discharge for the 7 cycles. The constructed cell exhibits the initial voltage of 0.32 V before charging (Fig. 7b). On continuous charging and discharging, at the 4^{th} cycle after the 2 h of charging, highest voltage of 2.27 V is observed.

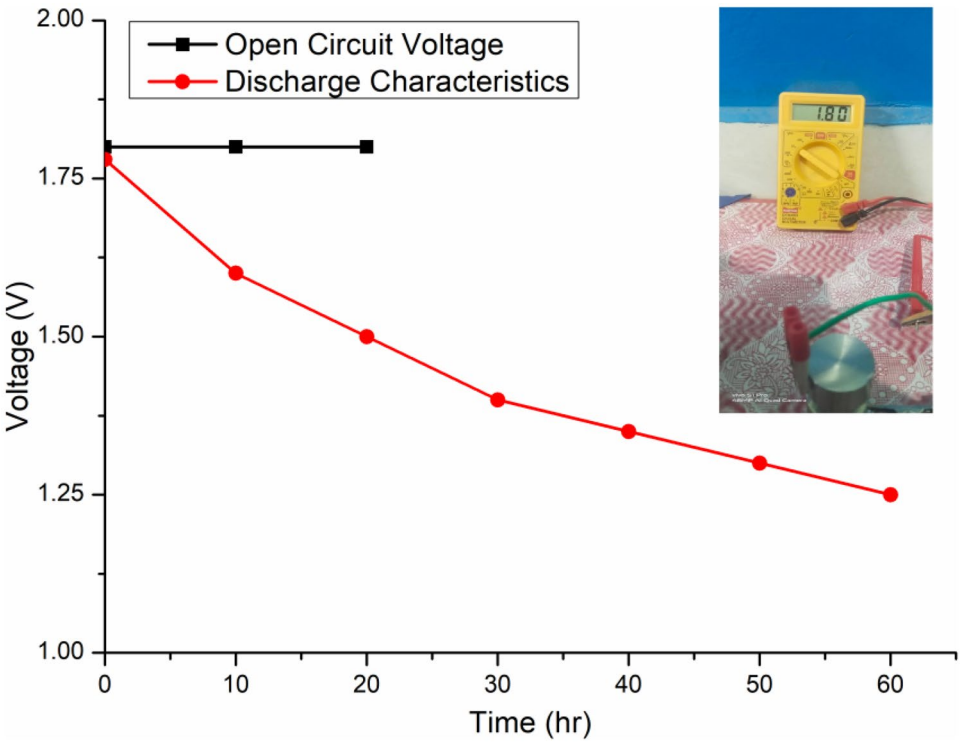

Fig. 6 OCV and discharge characteristic curve for the cell having the highest conducting electrolyte (1 g GG: 0.9 M.wt % of NH_4HCO_2). Inset: OCV value

Figure S8 represents the variation of resistance for different cycles. As the interfacial resistance at the anode increase, the charging capacity of the cell decrease with time. Figure S9a–d represent the discharge characteristics of the cell for various loads, 100 Ω, 1 kΩ, 47 kΩ and 100 kΩ respectively.

The charging and discharging characteristics of this proton cell at room temperature assure that the polymer electrolyte could be used for rechargeable proton battery.

Construction of single stack PEM fuel cell

On following the construction of Monisha et al. [15], the PEM Fuel cell has been constructed. The PEM fuel cell consist of hand tightened membrane electrode assembly (MEA), thin gaskets, bipolar graphite plates, copper plates, teflon sheets and stainless steel plates. The various parts of fuel cell are shown in the Fig. S10a. The stainless steel base plate and the copper plate are separated by Teflon sheet, which acts as an insulator. The copper plates are generally the current collectors that have poor corrosion resistance and good electrical and thermal conductivity; hence they are used in PEM fuel cells [39]. The bipolar graphite plate is kept over the copper plate. The bipolar graphite plate has the serpentine flow channel [39] of size 7.84 cm^2. The hand tightened membrane electrode assembly has been assembled with the highest conducting polymer electrolyte (1 g GG: 0.9 M.wt % of NH_4HCO_2) in between the platinum coated carbon cloth in which the platinum has been coated uniformly at the rate of 0.3 mg/cm^2 which acts a catalyst. This platinum coated carbon cloth of area ~ 8.41 cm^2 acts as the catalyst layer for the chemical reaction. This MEA has been sandwiched between the bipolar graphite plates with the gaskets of thickness 0.2 mm. The gaskets have been used to tighten the MEA with bipolar graphite plates for the air free flow. The assembled single stack PEM fuel cell has been shown in the Fig. S10b.

The hydrogen and oxygen gases have been produced using the electrolyser (Fig. S10c). It is operated under a DC voltage supply of 3 V. From this electrolyser, 100 ml of hydrogen and 80 ml of oxygen has been passed into the PEM fuel cell. When the hydrogen molecule passes through the platinum coated carbon catalyst, it is broken into proton and electron. The electron passes through the external circuit. The proton passes through the membrane and reaches the other side, where the oxygen molecule is broken and it combines with proton to form water. We get a pollution free current and the pure water as byproduct. The overall reaction of the PEM fuel has been represented below.

$$Anode\ reaction: 2H_2 \rightarrow 4H^+ + 4e^-$$

$$Cathode\ reaction: O_2 + 4H^+ + 4e^- \rightarrow 2H_2O$$

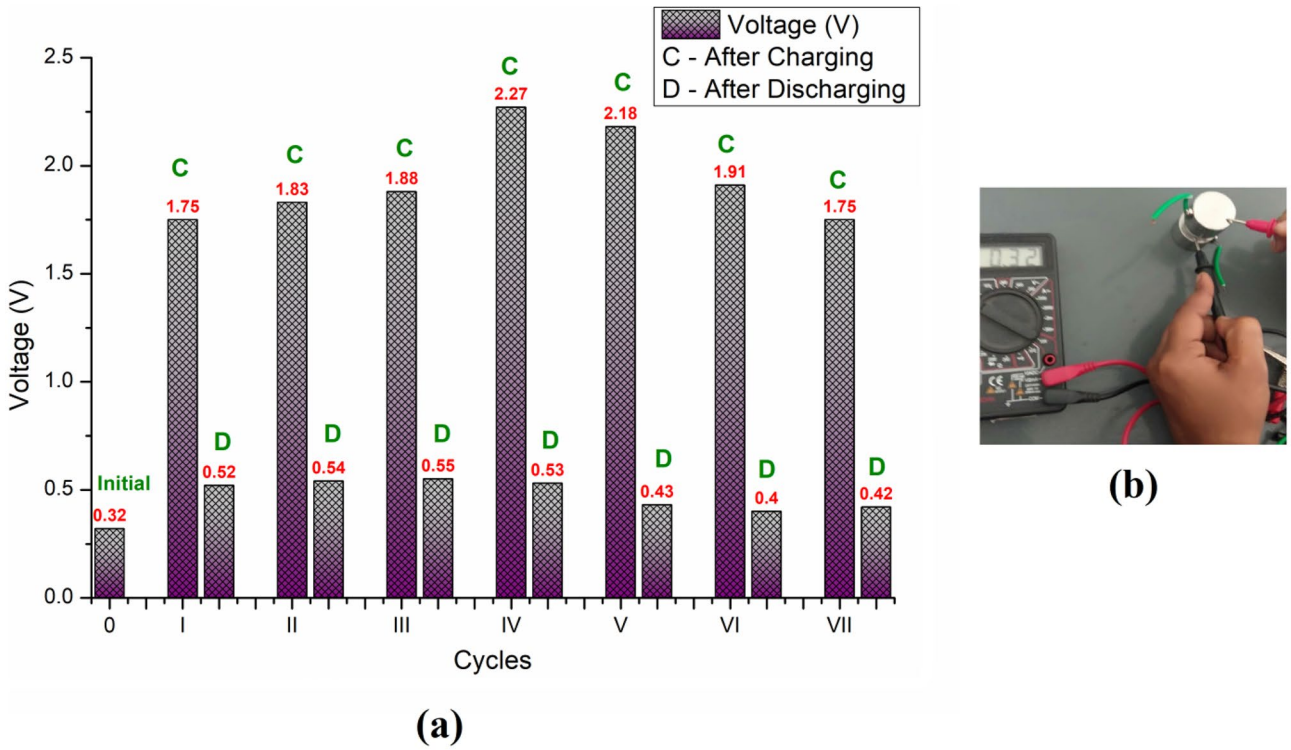

Fig. 7 **a** Charge and discharge cycles for the Rechargeable proton battery with highest conducting biopolymer electrolyte (1 g GG: 0.9 M.wt % of NH_4HCO_2) **b** Initial voltage of the rechargeable proton cell before charging

Overall reaction : $2H_2 + O_2 \rightarrow 2H_2O$

The PEM fuel cell constructed using 1 g GG: 0.9 M.wt % of NH_4HCO_2 exhibits the open-circuit voltage of 763 mV. Figure 8a represents the open circuit potential of PEM fuel cell. At this same condition, the PEM fuel cell using Nafion™ 212 proton exchange membrane has been constructed and the results were compared. The OCV of 758 mV has been obtained for Nafion™ 212 membrane Fig. 8b.

Various loads of 1 kΩ, 620 Ω, 270 Ω and 10 Ω have been connected as load across the both the PEM fuel cells (1 g GG: 0.9 M.wt % of NH_4HCO_2 and Nafion™ 212 membranes). The voltage and the corresponding current drawn are measured and plotted as graph (Fig S11a, b).

Monisha et al. has reported OCV of 656 mV for Cellulose acetate incorporated with ammonium nitrate [15]. The fuel cell constructed using biopolymer Agar: NH_4NO_3 showed the OCV of 558 mV [18]. Selvalakshmi et al. reported OCV of 500 mV for NH_4Br doped Agar polymer [20]. Moniha et al. has reported OCV of 442 mV for i- carrageenan with NH_4NO_3 [40]; similarly for i- carrageenan with NH_4SCN is 503 mV [41]. Meera Naachiyar et al. has reported OCV of 580 mV for GG biopolymer incorporated NH_4SCN [6].

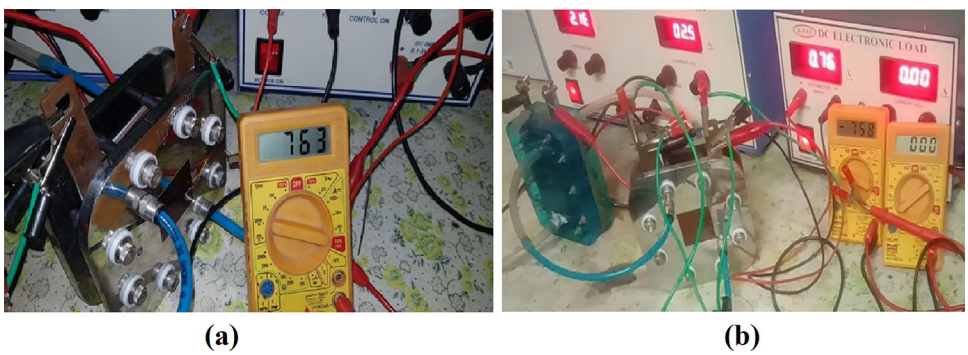

Fig. 8 **a** OCV of single PEM fuel cell constructed using **a** 1 g GG: 0.9 M.wt % of NH_4HCO_2 electrolyte **b** Nafion™ 212 membrane

Conclusion

The highest conducting polymer electrolyte (1 g GG with 0.9 M.wt % of NH_4HCO_2) has been prepared using the solution casting technique, which shows the conductivity of $5.62 \pm 0.09 \times 10^{-3}$ S/cm. The structural analysis of this electrolyte shows the amorphous nature with less crystallinity percentage (7.12%) and low glass transition temperature (44.12 ℃). The variation in force constant values indicates the change in bond length of the molecules exhibits the interaction of salt with the polymer matrix. The performance of biopolymer electrolyte in primary battery, secondary battery and PEM fuel cell has been analyzed and highest cell potential of 1.78 V, 2.27 V and 763 mV has been observed. The results compared with the earlier reports revels the Gellan gum biopolymer incorporated Ammonium Formate salt as promising electrolyte that may provide sustainable model to allow greener electrochemical device fabrication with improved electrochemical performance.

Supplementary Information The online version contains supplementary material available at https://doi.org/10.1007/s10965-022-03190-4.

Declarations

Conflict of interest Authors have no conflict of interest.

References

1. Subba Reddy CV, Sharmanad AK, Narasimha Rao VVR (2004) Characterization of a solid state battery based on polyblend of (PVP+PVA+KBr O3) electrolyte. Ionics 10:142–147
2. Meng C, Liu C, Chen L, Hu C, Fan S (2010) Highly flexible and all-solid-state aer like polymer super capacitors. Nano Lett 10:4025–4403
3. Fang J, Qiao J, Wilknson DP, Zhang J (eds) (2015) Electrochemical polymer electrolyte membranes. CRC Press, New York
4. Hassan M, Azimi N (2019) Conductivity and transport properties of starch/glycerin-MgSO4 solid polymer electrolytes. Int J Adv Appl Sci 6:38–43
5. Chitra R, Sathya P, Selvasekarapandian S, Monisha S, Moniha V, Meyvel S (2019) Synthesis and characterization of iota-carrageenan solid biopolymer electrolytes for electrochemical applications. Ionics 25:2147–2157
6. Naachiyar R, Ragam M, Selvasekarapandian S, Krishna M, Buvaneshwari P (2021) Development of biopolymer electrolyte membrane using Gellan gum biopolymer incorporated with NH4SCN for electro-chemical application. Ionics 27:3415–3429
7. Vanitha N, Shanmugapriya C, Subramanian S, Krishna M, Vengadesh N, Karuppasamy, (2022) Investigation of N-S-based graphene quantum dot on sodium alginate with ammonium thiocyanate (NH4SCN) biopolymer electrolyte for the application of electrochemical devices. J Mater Sci Mater Electron 33:1–21
8. Majid SR, Sabadini RC, Kanicki J, Pawlicka A (2014) Impedance analysis of gellan gum-poly (vinyl pyrrolidone) membranes. Mol Cryst Liq Cryst 604(1):84–95
9. Noor IM, Majid SR, Arof AK, Djurado D, Neto SC, Pawlicka A (2012) Characteristics of gellan gum–LiCF3SO3 polymer electrolytes. Solid State Ion 225:649–653
10. Noor IM (2020) Determination of charge carrier transport properties of gellan gum–lithium triflate solid polymer electrolyte from vibrational spectroscopy. High Perform Polym 32:168–174
11. Neto MJ, Sentanin F, Esperança J, Medeiros MJ, Pawlicka A, Bermudez V, Silva M (2015) Gellan gum—ionic liquid membranes for electrochromic device application. Solid State Ion 274
12. Rahul S, Bhaskar B, Hee-Woo R, Pramod S (2015) Solid gellan gum polymer electrolyte for energy application. Int J Hydrogen Energy 40:9365–9372
13. Karthika J, Vishalakshi B, Jagadish N (2015) Gellan gum–graft–polyaniline—an electrical conducting biopolymer. Int J Biol Macromol 82:61–67
14. Abdul Halim NF, Majid SR, Arof AK, Kajzar F, Pawlicka A (2012) Gellan gum-LiI gel polymer electrolytes. Mol Cryst Liq Cryst 554:232–238
15. Monisha S, Mathavan T, Selvasekarapandian S, Milton Franklin Benial A, Aristatil G, Mani N, Premalatha M, Vinoth Pandi D (2017) Investigation of bio polymer electrolyte based on cellulose acetate-ammonium nitrate for potential use in electrochemical devices. Carbohydr Polym 157:38–47
16. Moniha V, Marimuthu A, Selvasekarapandian S, Sundaresan B, Hemalatha R (2019) Development and characterization of biopolymer electrolyte iota-carrageenan with ammonium salt for: electrochemical application. Mater Today Proc 8:449–455
17. Karthikeyan S, Selvasekarapandian S, Premalatha M, Monisha S, Boopathi S, Aristatil G, Arun A, Saminathan M (2017) Proton-conducting I-Carrageenan-based biopolymer electrolyte for fuel cell application. Ionics 23:2775–2780
18. Boopathi G, Pugalendhi S, Selvasekarapandian S, Premalatha M, Monisha S, Aristatil G (2017) Development of proton conducting biopolymer membrane based on agar–agar for fuel cell. Ionics 23:2781–2790
19. Selvalakshmi S, Mathavan T, Selvasekarapandian S, Premalatha M (2018) A study of electrochemical devices based on Agar-Agar-NH4I biopolymer electrolytes. AIP Conference Proceedings 140019
20. Selvalakshmi S, Mathavan T, Selvasekarapandian S et al (2019) Characterization of biodegradable solid polymer electrolyte system based on agar-NH_4Br and its comparison with NH_4I. J Solid State Electrochem 23:1727–1737
21. Premalatha M, Mathavan T, Selvasekarapandian S, Selvalakshmi S, Monisha S (2017) Incorporation of NH4Br in tamarind seed polysaccharide biopolymer and its potential use in electrochemical energy storage devices. Org Electron 50:418–425
22. Premalatha M, Mathavan T, Selvasekarapandian S, Selvalakshmi S (2018) Structural and electrical characterization of tamarind seed polysaccharide (TSP) doped with NH4HCO2. AIP Conference Proceedings 070005
23. Mohamed A, Abd. Shukur M, Kadir M, Yusof Y (2020) Ion conduction in chitosan-starch blend based polymer electrolyte with ammonium thiocyanate as charge provider. J Polym Res 27(6)
24. Hodge RM, Edward GH, Simon GP (1996) Water absorption and states of water in semicrystalline poly(vinyl alcohol) films. Polymer 37(8):1371–1376
25. Vinoth Pandi D, Selvasekarapandian S, Bhuvaneswari R, Premalatha M, Monisha S, Arun Kumar D, Kawamura J (2016) Development and characterization of proton conducting polymer electrolyte based on PVA, amino acid glycine and NH4SCN. Solid State Ion 298:15–22
26. Premalatha M, Mathavan T, Selvasekarapandian S, Monisha S, Vinoth Pandi D, Selvalakshmi S (2016) Investigations on proton conducting biopolymer membranes based on tamarind seed polysaccharide incorporated with ammonium thiocyanate. J Non-Cryst Solids 453:131–140

27. Boukamp BA (1986) A nonlinear least squares fit procedure for analysis of immittance data of electrochemical systems. Solid State Ion 20(1):31–44
28. Machado GD, Regiani AM, Pawlicka A (2003) Carboxymethylcellulose derivatives with low hydrophilic properties. Polimery 48(4):273–279
29. Mollá S, Compañ V (2011) Polyvinyl alcohol nanofiber reinforced Nafion membranes for fuel cell applications. Energy Fuels 372:191–200
30. Muthukrishnan M, Shanthi C, Selvasekarapandian S, Shanthi G, Sampathkumar L, Maheshwari T (2021) Impact of ammonium formate (AF) and ethylene carbonate (EC) on the structural, transport and electrochemical properties of pectin based biopolymer membranes. Ionics 27:3443–3459
31. Chenliang Gong Yu, Liang ZQ, Li H, Zhongying Wu, Zhang Z, Zhang S, Zhang X, Li Y (2015) Solution processable octa(aminophenyl)silsesquioxane covalently cross-linked sulfonated polyimides for proton exchange membranes. J Membr Sci 476:364–372
32. Yang T, Li Z, Lyu H, Zheng J, Liu J, Liu F, Zhang Z, Rao H (2018) A graphene oxide polymer brush based cross-linked nanocomposite proton exchange membrane for direct methanol fuel cells. RSC Adv 8(28):15740–15753
33. Pasquini L, Zhakisheva B, Sgreccia E, Narducci R, Di Vona ML, Knauth P (2021) Stability of proton exchange membranes in phosphate buffer for enzymatic fuel cell application: Hydration, conductivity and mechanical properties. Polymers (Basel) 13(3):475
34. Zhao C, Lin H, Shao K, Li X, Ni H, Wang Z, Na H (2006) Block sulfonated poly(ether ether ketone)s (SPEEK) ionomers with high ion-exchange capacities for proton exchange membranes. J Power Sources 162:003–1009
35. Pandey K, Lakshmi N, Chandra S (1998) A rechargeable solid state proton battery with an intercalating cathode and an anode containing a hydrogen storage-material. J Power Sources 76(1):116–123
36. Tamilarasan K, Selvasekarapandian S, Chitra R, Kiruthika S (2021) Investigation of blend biopolymer electrolytes based on Dextran-PVA with ammonium thiocyanate. J Solid State Electrochem 25:1–11
37. Hemalatha R, Marimuthu A, Selvasekarapandian S, Sundaresan B, Moniha V (2019) Studies of proton conducting polymer electrolyte based on PVA, amino acid proline and NH4SCN. J Sci Adv Mater Dev 4:101–110
38. Hemalatha R, Alagar M, Selvasekarapandian S, Sundaresan B, Moniha V, Boopathi G, Christopher S (2019) Preparation and characterization of proton-conducting polymer electrolyte based on PVA, amino acid proline, and NH4Cl and its applications to electrochemical devices. Ionics 25:141–154
39. Tang Y, Yuan W, Pan M, Wan Z (2010) Feasibility study of porous copper fiber sintered felt: A novel porous flow field in proton exchange membrane fuel cells. Int J Hydrogen Energy 35:9661–9677
40. Moniha V, Alagar M, Selvasekarapandian S, Sundaresan B, Boopathi G (2017) Conductive bio-polymer electrolyte iota-carrageenan with ammonium nitrate for application in electrochemical devices. J Non-Cryst Solids 481:424–434
41. Moniha V, Alagar M, Selvasekarapandian S, Sundaresan B, Hemalatha R, Boopathi G (2018) Synthesis and characterization of bio-polymer electrolyte based on iota-carrageenan with ammonium thiocyanate and its applications. J Solid State Electrochem 22:1–15